Following the trails of India's Atmospheric Lead (Pb): Source Identification, Apportionment, Bioavailability and Remediation

SYNOPSIS SUBMITTED

FOR THE DEGREE OF

DOCTOR OF PHILOSOPHY (ENGINEERING)

To

JADAVPUR UNIVERSITY

2025

By

IRAVATI RAY

Registration No.: 1022220001 of 2022

SCHOOL OF ENVIRONMENTAL STUDIES

JADAVPUR UNIVERSITY, KOLKATA: 700032, INDIA

TABLE OF CONTENTS

CHAPTER 1: INTRODUCTION

Air pollution has been a persistent issue since ancient times, with its effects on health and the environment documented as early as 400 BCE by Hippocrates (Hippocrates, 400BCE). Over centuries, both natural and anthropogenic sources have contributed to air quality deterioration, with industrialization in the 18th and 19th centuries amplifying the problem. The emergence of coal as a dominant fuel source introduced "smog" and other pollutants, resulting in public health crises and legislative actions globally (Corton, 2021; Fowler et al., 2020). Despite these interventions, air pollution remains a significant challenge in the modern era, particularly in developing countries.

Particulate matter (PM), a mixture of solid particles and liquid droplets suspended in the air, is a critical component of air pollution with wide-ranging impacts. PM is categorized into coarse particles (PM_{10}) and fine particles ($PM_{2.5}$), with the latter being particularly concerning due to its ability to penetrate deep into the respiratory tract and bloodstream, leading to severe health outcomes such as respiratory and cardiovascular diseases, cancer, and premature death (Guevara, 2016; Roser, 2021). Globally, $PM_{2.5}$ is responsible for millions of deaths annually, The World Health Organization estimating that 99% of the population lived in areas exceeding air quality guidelines in 2019 (WHO, 2024).

In India, the problem is particularly acute due to rapid industrialization and urbanization. Major contributors to PM pollution include vehicular emissions, coal combustion, industrial processes, and agricultural residue burning, especially in northern states like Punjab and Haryana. Seasonal practices such as stubble burning exacerbate pollution levels in cities like Delhi, where $PM_{2.5}$ concentrations frequently exceed recommended limits and shoot up to hazardous levels. India's reliance on fossil fuels for energy production further contributes to the issue, with coal-fired power plants emitting significant amounts of particulate-bound toxic metals (Bhuvaneshwari et al., 2019; Chatterjee et al., 2023; Roser, 2021; Venkataraman et al., 2018).

Among the various pollutants associated with PM, lead (Pb) is especially concerning due to its toxicity and persistence in the environment. Although the phase-out of leaded gasoline has significantly reduced Pb emissions globally, atmospheric Pb remains persistent in India due to other anthropogenic activities. Pb is a non-essential toxic metal linked to severe health risks,

including developmental issues in children. Recent studies reveal alarmingly high blood Pb levels among Indian children, with millions exceeding safe limits, leading to significant cognitive and health impairments (UNICEF and Pure Earth, 2020).

Pb isotopes (^{204}Pb, ^{206}Pb, ^{207}Pb, and ^{208}Pb) along with elemental concentrations provide a powerful tool for tracing pollution sources due to their unique isotopic signatures (Komárek et al., 2008). In India, isotopic studies have identified coal combustion, industrial emissions, and transported dust as key contributors to atmospheric Pb (Bollhöfer and Rosman, 2001; Das et al., 2018; Kumar et al., 2018, 2016; Mitra et al., 2021; Sen et al., 2016). However, the contribution of multiple sources remains inadequately studied. This gap highlights the need for comprehensive investigations to delineate and quantify the sources.

Thus, this research focuses on identifying and quantifying the sources of atmospheric Pb in India using isotopic and elemental analyses. It also explores atmospheric Pb mitigation strategies, using ferns, which have demonstrated significant potential in capturing PM bound metal pollutants.

CHAPTER 2: MATERIALS AND METHODS

2.1. Collection of PM_{10} and $PM_{2.5}$ aerosol samples and dustfall (DF) samples

The PM_{10} aerosol samples at Kolkata were collected for 14 days using a personal modular impactor PM_{10} (PMI, SKC Inc., USA) connected to a Deployable Particulate Sampler (DPS, Leland Legacy Pump, SKC Inc., USA) with a pumping efficiency of 10L/min. At Andaman and Nicobar Islands PM_{10} and $PM_{2.5}$ aerosol samples were collected by a two-stage inertial SKC IMPACT $PM_{10\text{-}2.5}$ and $PM_{2.5}$ sampler (SKC Inc., USA) connected to a Deployable Particulate Sampler (DPS, Leland Legacy Pump, SKC Inc., USA) with a pumping efficiency of 10 L/min. The PM_{10} samples were collected upon 47mm Polytetrafluoroethylene (PTFE) filters. At Neyveli the $PM_{2.5}$ sampling was performed with Envirotech APM 550 MFC sampler at a constant flow rate of 1 m^3/hr. The samples were collected in pre-weighed 46.2mm Whatman PTFE filters with a pore size of 2 μm. All filter papers for aerosol sample collection were pre-washed with 1N HCl at 140°C before being rinsed several times with ultrapure water. The filters were dried in an oven at 60°C, weighed, and sealed in pre-cleaned petri dishes before sampling. The samplers were placed on the roofs of buildings approximately 12 m above ground level (AGL). The concentrations of PM were determined gravimetrically by weighing then after sampling.

Dust fall samples were collected on acid washed polystyrene Petri dishes (90 mm diameter) exposed for 7 days. Pre-weighed petri dishes (n = 6) were fixed on roofs of buildings using double sided tapes to avoid any disturbance due to wind during dust settling (Gulson et al., 1995). No rainfall event occurred during the period of sampling. The petri dishes were sealed and kept inside airtight zipper bags before being processed for analysis.

2.2. Collection and pre-processing of traffic emission samples

All the traffic emission samples were collected from different locations in the city of Kolkata. The surfaces of the collected tire segments (n = 5) and brake pads (n = 3) were collected from local car repairing shops. sonicated in Milli-Q water to remove loose contaminants. Following cleaning, the tires were cut and homogenized into small pieces. The brake pads were scraped to generate loose homogenized brake wear particles. Samples of yellow and white road paint (n = 2) were applied and dried on polypropylene sheets, following which they were scraped off as dry particles (Jeong

et al., 2022). Road pitch samples (n = 7) were collected from road, crushed and homogenized into finer particles. Vehicular exhaust samples (both petrol and diesel) (n = 5), along with vehicular exhaust from tailpipes, were also collected. The soot from tailpipes were scrapped off using plastic knifes directly into Ziploc bags.

2.3. Collection of vehicular and ship fuel samples

Vehicular fuel samples of petrol and diesel (n = 5) were collected rom petrol pumps in Kolkata. High-speed diesel, along with lubricant samples (15W40, OMD 113) from the gearbox, and coolant samples (Havoline and Primax), were collected as ship oil samples. A total of three diesel samples, five lubricant samples, and three coolant samples were obtained for analysis. The engine was of a large survey vessel named Sandhayak with 4 strokes and 9 cylinders, built and maintained by Garden Reach Shipbuilders & Engineers Limited (GRSE). The engine has 270 mm bore and 380 mm stroke size and operates at a speed of 800 rpm with a maximum power of 3285 kW.

2.4. Collection and pre-processing of fern and associated samples

Pteris vittata and *Pteridium aquilinum* were observed to be widely distributed species of ferns throughout the region. Both species were sampled from 12 sites, from about 1 – 1.5 m above the ground. All the plants were in good condition and none were shaded by overhead vegetation, ensuring that the leaves were fully exposed to the atmospheric fallouts. Leaves were hand-plucked and samples from each site were sealed in separate acid-washed plastic containers to prevent cross contamination and minimize PM loss from the leaf surface. The roots of corresponding plants along with the rhizosphere soils of individual sample were sealed in separate ziploc bags. Plants of similar age determined by their appearance (height, sori development) and identified by surveying local people were selected for the study. Samples were collected at each site on the same days under rainless conditions.

2.4.1. Gravimetric quantifications and determination of leaf surface area

Foliar dusts were categorized as: (i) Loose dust (LD) and (ii) Wax bound dust (WD). The loads of dust on the leaves were determined gravimetrically using washing and weighing method (Dzierżanowski et al., 2011). A total of 22 leaves were weighed and submerged in ultrapure water (Resistivity = 18 MΩ.cm) in a 50 mL centrifuge tube and hand-shaken for 10 mins to remove the LD. The same leaf was removed from the water and submerged in trace metal grade chloroform

in a separate pre-weighed Teflon beaker and shaken for 10 mins to remove the WD. The water was transferred into pre-weighed Teflon beakers and both the water and chloroform were evaporated. After evaporation the beakers were reweighed to quantify the amount of LD and WD captured by each leaf. The cleaned leaves were photographed against a white backdrop and a digital file was created. The images were analyzed by Image-J software to calculate the individual leaf surface areas (O'Neal et al., 2002). The cleaned leaves, roots and rhizosphere soils were dried at 60 °C until constant weight and ground in agate mortar and pestle for further processing.

2.4.2. Microscopic observations of leaf-surface PM by SEM-EDX

A dusty leaf from each species were dried at 60°C until constant weights. The samples were sputter coated with platinum. The adaxial and abaxial surface PM of the leaves were examined using the ESEM (SEM: ZEISS EVO-MA 10; Carl Zeiss Pvt. Ltd., Oberkochen, Centre for Research in Nanoscience and Nanotechnology, University of Calcutta) at 500x and 200x magnifications. Energy Dispersive X-Ray Analysis (EDX) (SmartEDX, Carl Zeiss) was performed to observe the elemental content of elements present on the surface of the leaves.

2.5. Sample processing for extraction of elements

All samples were processed in clean chemistry laboratory using Milli-Q water, having resistivity > 18.2 MΩ-cm and acids purified by sub-boiling distillation of concentrated reagent grades.

2.5.1. PM_{10} and $PM_{2.5}$ aerosol and dustfall samples

The aerosol and dustfall samples were subjected to hot plate digestion in screw cap Teflon beakers (Savillex^{TM}) for 24 hours at 120°C in a mixture of concentrated 3:1 HNO_3 and HF. The digested samples were evaporated to dryness. The dried samples were redissolved and refluxed twice in concentrated HNO_3 to remove traces of HF. The solutions were dried down and redissolved in 2 mL of 2 % HNO_3, half of which was utilized for determination of elemental concentration and the other half was stored for performing anion exchange chromatography to separate Pb.

2.5.2. Lignite, fly ash, soil, solid waste ash, biomass burning ash and galena samples

Initially, the lignite samples were ashed in a muffle furnace at 300°C for 1 hour and 500°C for the next two hours before subjecting them to acid digestion (Díaz-Somoano et al., 2009). About 20

mg of the ashed lignite, top soil, SW burning ash, biomass burning ash, fly ash samples were weighed and subjected to hot plate acid digestion for 24 hours at 120°C in a mixture of concentrated 3:1 HNO_3 and HF. The digested samples were evaporated to dryness. The dried samples were redissolved and refluxed twice in concentrated HNO_3 to remove traces of HF. The solutions were dried down and redissolved in 2 mL of 2 % HNO_3, half of which was utilized for determination of elemental concentration and the other half was stored for performing anion exchange chromatography to separate Pb.

2.5.3. Brake wear, tire wear, vehicular exhaust, road pitch and road dust samples

The homogenized brake wear, tire wear, road pitch, and road paint samples were weighed (~30 mg) and digested for 24 hours at 120°C in screw cap Teflon beakers (Savillex^{TM}) using a concentrated acid mixture of HNO_3 and H_2O_2 in 2:1 ratio. The vehicular exhaust samples were digested in concentrated HNO_3 at 120°C for 24 hrs in screw cap Teflon beakers (Savillex^{TM}). The solutions were dried down and redissolved in 2 mL of 2 % HNO_3, half of which was utilized for determination of elemental concentration and the other half was stored for performing anion exchange chromatography to separate Pb.

2.5.4. Vehicular and ship fuel samples

The ship and vehicular oil samples (1 mL each) were ashed using a muffle furnace in high-temperature-resistant Pyrex tubes, plugged with quartz wool. Prior to use, the Pyrex tubes were acid-washed. The ashing process was conducted at approximately 500°C for several hours until visible ash residues accumulated at the bottom of the tubes. To prevent combustion, the temperature was gradually increased in small increments throughout the process (10°C every 5 mins). The ashes were digested in a mixture of aqua regia and hydrogen peroxide (1:1) (Sugiyama and Williams-Jones, 2018). All the digested samples were evaporated to dryness. The dried samples were then dissolved in 2 mL of 2% HNO_3, with one half used for elemental concentration analyses and the other half reserved for anion exchange chromatography to isolate Pb.

2.5.5. Fern and associated samples

All samples were digested in Teflon beakers at 120 °C using different mixtures of acid necessary for maximum elemental extractions as reported in **Table 2.1**.

***Table 2.1**: Digestion mixtures used for different types of samples*

Sample Type	Acid Mixture	References
PM_{10} aerosols	HNO_3 : HF = 50% of 3 : 1	(Kayee et al., 2021); USEPA 3052, 1996)
Dust fall	HNO_3 : HF = 3 : 1	
Loose dusts	HNO_3 : HF = 3 : 1	
Wax bound dusts	Aqua regia : H_2O_2 = 1: 1 followed by HNO_3 : HF = 3 : 1	
Cleaned leaves	HNO_3 : H_2O_2 = 2 : 1	(Lamble and Hill, 1998)
Roots	HNO_3 : H_2O_2 = 2 : 1	(Lamble and Hill, 1998) USEPA 3052, 1996
Soils	HNO_3 : HF = 3 : 1	

The WDs were subjected to iterative treatment using HCl, HNO_3 and H_2O_2 to fully digest the wax. The sequential leaching steps for the selected soil sample included reflux of dried leached fractions in concentrated HNO_3 after extraction of (i) exchangeable fraction (SE) by 1 M Sodium Acetate at pH 7.8; (ii) carbonate fraction (SC) by 1 M Sodium Acetate adjusted to pH 5 with Acetic acid; (iii) reducible/Fe-Mn fraction (SR) in 0.04 M Hydroxylamine hydrochloride dissolved in 25% (v/v) acetic acid; and (iv) dissolution of silicate fraction (SS) in concentrated Nitric and Hydrofluoric acid mixture (3:1) (Tessier et al., 1979).

The acid mixtures for all types of samples were evaporated following digestion for 24 h. The samples containing HF were refluxed twice using concentrated HNO_3 and evaporated to remove any traces of HF. Finally, the dried samples were dissolved in 2 mL of gravimetrically prepared 2% HNO_3. From this 2 mL, half was utilised for concentration analyses and the other half for Pb isotope determination.

2.6. Sample processing for purification of Pb

For separation of Pb, the samples in 2 % HNO_3 were dried down and redissolved in ultrapure 1.1 N HBr. The column elution acids were 1.1 N HBr, 2 N and 6 N HCl which were prepared volumetrically and titrated against 1.0 N NaOH to determine their exact normality. Elution was performed in shrinkable Teflon columns packed till neck with pre-cleaned anion exchange resin (Eichrom AG-1X8 chloride form, 200 – 400 mesh). The resin cleaning process involved sequential

centrifugation at 3000 rpm for 6 minutes first in Milli-Q water, followed by 2 N HCl and subsequently with 6 N HCl. The columns were fitted with acetate membrane frits. The column-loaded resin is cleaned by passing double-distilled 6 N HCl twice. The columns filled with resin were conditioned with 400 µL of 1.1 N HBr before loading the samples (100 – 200 µL). This step was followed by elution using 600 µL of 1.1 N HBr and 400 µL of 2 N HCl. Finally Pb was eluted in 600 µL of 6N HCl (Reuer et al., 2003). The Pb eluted in HCl was evaporated and redissolved in 2 % HNO_3.

2.7. Determination of elemental concentrations

All aerosol and DF samples from Neyveli, Andaman and Nicobar Islands and end member samples including, lignite, fly ash, solid waste and biomass burning ash, soil, galena, chalcopyrite road emission samples were analysed using the Thermo Scientific iCAP Q ICP-MS at Earth Observatory of Singapore, Nanyang Technological University, Singapore. For elements having high concentrations in the road emission samples (Al, Ba, Ca, Fe, Mg, Mn, Cu and Zn), measurements were initially performed on an Thermo Scientific^{TM} iCAP 7000 inductively coupled plasma - optical emission spectrometer (ICP – OES) at the Paleothermometry Laboratory of National Centre for Polar and Ocean Research (NCPOR), Goa, India. For standard sample bracketing, a multi element standard (Merck ICP ME IV) of 5 ppm was used. The obtained intensities of the samples were drift corrected and normalized with respect to the intensity of the bracketing standard.

The sample introduction setup for iCAP Q ICP-MS included a Peltier cooled quartz cyclonic spray chamber, a PFA concentric nebulizer (100µL/min), and a demountable quartz torch with a quartz injector. Platinum sampler and skimmer cones were employed at the quadrupole – torch interface. All the samples and standards were diluted in 2 % HNO_3. The instrument was operated in a single collision cell mode with kinetic energy discrimination (KED), employing pure helium (He) as the collision cell gas to remove polyatomic interferences. The instrument was tuned in iCAP Q tuning solution comprising of 1 µg/L of Ba, Bi, Ce, Co, In, Li and U. Multi element calibration standards ranging from 0.1 ppb to 500 ppb were freshly prepared gravimetrically and analyzed to obtain linear calibration curves. A multi element standard of 10 ppb was used for standard – sample bracketing. Drift corrections and normalization of the obtained raw counts per second (cps) were performed with respect to the bracketing standard.

All the PM_{10} aerosol samples from Kolkata and fern and associated samples were initially measured for elements having high concentrations (Al, Ba, Ca, Fe, Mg, and Mn) on an Agilent 5800 Inductively coupled plasma - optical emission spectrometer (ICP – OES). Analytes having lower concentrations (Ti, V, Cr, Ni, Co, Cu, Cd and Pb) were measured on an Agilent 8900 Triple Quadrupole Inductively coupled Plasma Mass Spectrometer (ICP – MS, Agilent Technologies, Santa Clara, CA, USA). Thus, concentrations of 14 elements (Mg, Al, Ca, Ti, V, Cr, Mn, Fe, Co, Ni, Cu, Cd, Ba, and Pb) were determined for all the samples using the above – mentioned instruments at Centre for Earth Sciences, Indian Institute of Science, Bangalore.

The sample introduction system of the ICP – OES includes a peristaltic pump, with a micro mist concentric nebulizer (800-900 µL/ min), and a quartz double pass spray chamber. The wavelengths selected for the analytes on the ICP – OES had the highest sensitivity and lowest spectral interferences from other elements. Multi-element calibration standards ranging from 0.1 ppm to 20 ppm were freshly prepared gravimetrically and analysed. A multi-element standard of 1 ppm was utilised for standard – sample – standard bracketing. Drift corrections and normalisations of the raw data were performed with respect to the intensities of the bracketing standard.

The sample introduction system of Agilent 8900 Triple Quadrupole Inductively coupled Plasma Mass Spectrometer consists of self-aspirating ESI nebulizer (uptake rate 100 µL/min), temperature controlled (+2°C) scott type quartz spray chamber, quartz torch and nickel sampler and skimmer cones. All the samples were diluted in 1ppb Y doped 2% HNO_3. Concentrations were measured in hot plasma in collision reaction cell (CRC) mode to remove the polyatomic interferences. Two sets of multi-element calibration standards ranging from 0.1 ppb to 20 ppb were freshly prepared gravimetrically and analysed. A multi-element standard of 1 ppb was utilised for standard – sample – standard bracketing. Drift corrections and normalisations of the raw data were performed with respect to the counts per second (cps) of the bracketing standard. The procedural blanks were also analysed in ICP MS and were subtracted from the total concentration of the elements.

To determine the extraction efficiency and analytical precision, standard reference materials (SRM) from National Institute of Standards and Technology (NIST) were digested following procedures exactly same as similar types of samples.

2.8. Determination of Pb isotopes

Pb isotopes were analysed by Multi-collector ICP – MS (Neptune Plus MC ICP-MS, Thermo-Fisher, Germany) at Earth Observatory of Singapore, Nanyang Technological University, Singapore, equipped with Aridus II desolvating nebulizer (100 µL/min). Instrumental mass fractionation correction involved Thalium (Tl) (NIST SRM 997) internal normalisation ($^{203}Tl/^{205}Tl$ ratio of 0.418911). Bracketing with NIST SRM-981 was adopted to normalise the obtained ratios with respect to the true value (Baker et al., 2004; White et al., 2000).

All the samples were concentration matched with standard and anaysed at comparable Pb/Tl ratios, to minimize the mass bias generated from counting statistics. The precision and accuracy of the measurements were ensured by analysing NIST SRM-981 multiple times between samples as well as at the beginning and end of sessions. The contribution of the procedural blank to the total measured concentration were determined as [Pb]procedural blank/[Pb]Total. Consequently, the blank subtracted $^{206}Pb/^{207}Pb$ and $^{208}Pb/^{207}Pb$ values were determined by mass balance represented by the following equation (Gelwicks and Hayes, 1990):

$$\left(\frac{20x}{20y}\right)_{sample} = \left[n_T \left(\frac{20x}{20y}\right)_{total} - n_B \left(\frac{20x}{20y}\right)_{blank}\right] / (n_T - n_B) \quad \text{.....3.1}$$

Where, x = 6, 8; y= 7, 6; n is the fractional amount of substance and the subscripts T, and B refers to total and blank respectively.

2.9. Statistical analyses and modelling studies

2.9.1. Air mass back trajectory analyses

Air-mass back trajectory statistics were obtained using meteorological data for the sampling dates, extending up to 72 hours prior. The meteorology data, that included wind speed, wind direction, temperature, humidity, and precipitation, was compiled using the Hybrid Single-Particle Lagrangian Integrated Trajectory (HYSPLIT) model through its graphical user interface (GUI)(Draxler, 1998; NOAA, 2021). This meteorological data was provided as an input into the geographic information system (GIS) based software TrajStat to generate 72-hour airmass back trajectories at 500 meters above sea level. These trajectories were then converted into a polylineZ shapefile format for spatial representation(Wang et al., 2009).

2.9.2. Mixing polygon simulation

The mixing polygon simulation is conducted in Pb isotope space involving three ratios: $^{206}Pb/^{207}Pb$, $^{208}Pb/^{207}Pb$, and $^{208}Pb/^{206}Pb$. It assesses whether majority of the aerosol mixtures fall within the mixing envelope of the considered end members. It is a Monte Carlo simulation performed in R 4.2.2 (http://www.famer.unsw.edu.au/downloads.html). As inputs for sources of the aerosol mixtures the mean Pb isotopic compositions ($^{206}Pb/^{207}Pb$, $^{208}Pb/^{207}Pb$, and $^{208}Pb/^{206}Pb$ ratios or $^{206}Pb/^{204}Pb$, $^{207}Pb/^{204}Pb$ and $^{208}Pb/^{204}Pb$ ratios) along with 1 standard deviations (SD) of the sources were fed. The Pb isotopic compositions ($^{206}Pb/^{207}Pb$, $^{208}Pb/^{207}Pb$, and $^{208}Pb/^{206}Pb$ ratios or $^{206}Pb/^{204}Pb$, $^{207}Pb/^{204}Pb$ and $^{208}Pb/^{204}Pb$ ratios) of all the aerosols were fed to the model as mixture parameters. The model performs iterations (n = 1500) that generate mixing envelopes based on the distribution of the considered sources and their SDs. The number of such envelopes that include within them the aerosols, represent the probability of the aerosols for lying inside the mixing envelope (Smith et al., 2013). The mixing polygon simulation is based on the principle that the isotopic composition of the mixture (aerosols for this study) can be explained by the isotopic compositions of the sources forming the mixing envelope only if the mixture doesn't fall outside 5 % of the generated polygons. The sample(s) with less than 5 % probabilities has/ve sources other than the considered end members and hence the selected sources cannot explain the composition of that particular mixture.

2.9.3. Linear mixing model performed for literature data of India and SEA countries

The aerosol mixtures of India, and SEA countries from the past decade as compiled from previous literatures were primarily visualized along a two-end member geometric mixing line, partitioned into intervals of 20 %. The proximity of the aerosol mixture to each source on the line provides the relative contribution between the two considered sources (Phillips and Gregg, 2003). Since, such an approach cannot consider more than 2 sources, following this, the aerosol mixture and the source Pb isotopic data were subjected to conventional mass balance based linear mixing model based on the principle of IsoSource by employing the following equations (Phillips et al., 2005):

$$\left(\frac{206}{207}Pb\right)_{mix} = \left[f_a\left(\frac{206}{207}Pb\right)_a + f_b\left(\frac{206}{207}Pb\right)_b + \cdots + f_n\left(\frac{206}{207}Pb\right)_n\right] \quad \text{.....3.2}$$

$$\left(\frac{208}{207}Pb\right)_{mix} = \left[f_a\left(\frac{208}{207}Pb\right)_a + f_b\left(\frac{208}{207}Pb\right)_b + \cdots + f_n\left(\frac{208}{207}Pb\right)_n\right] \quad \text{.....3.3}$$

$$f_a + f_b + \cdots + f_n = 1 \quad \text{.....3.4}$$

where $\left(\frac{206}{207}Pb\right)_{mix}$ and $\left(\frac{208}{207}Pb\right)_{mix}$ are isotopic compositions of the aerosol mixtures; $\left(\frac{206}{207}Pb\right)_{a,b,\ldots,n}$ and $\left(\frac{208}{207}Pb\right)_{a,b,\ldots,n}$ are isotopic compositions of the sources and $f_{a,\ b,\ \ldots,\ n}$ is the unknown proportional contribution for each source towards the aerosol mixture. It is worth noting that these equations are approximations that work because of the limited fractional variance of Pb isotope data. This system using two isotope ratios can provide unique solution for each f, up to n = 3. However, when n > 3, this becomes an underdetermined system with no unique solution (Phillips and Gregg, 2003) To estimate the source proportions ($f_{a,\ b,\ \ldots,\ n}$) from such an underdetermined system, iterative approach as followed in traditional models like IsoSource was employed (Phillips and Gregg, 2003). The linear model was made to perform an optimization process to find the optimal value for mixture of sources that matches given target aerosol mixture values. The optimization process performs ten restarts, each starting with a set of randomly assigned initial values for source proportions for the five sources. This process of conducting 10 restarts in the model was repeated 10 times to yield a set of 10 distinct sets of best results. The goal is to achieve an average deviation of 0.5‰ or less between the predicted and target mixture values. Two target aerosol mixtures, one with most radiogenic signature and the other with least, were selected. This selection is based on the fact that the source contribution towards the aerosols, lying between these extremes, will fall within the range of source contributions obtained for these extreme target aerosols. The model then identifies the best solution based on the lowest deviation. The potential combinations of source proportions sum up to 100%. (Phillips and Gregg, 2003).

2.9.4. Bayesian mixing model, MixSIAR (Stable isotope analysis in R)

Bayesian statistics based mixing models integrates the mean and uncertainty of the data into its framework. It is based on Markov Chain Monte Carlo (MCMC) simulation that produces plausible source proportion results based upon probability densities of the fed data (Parnell et al., 2010). This is particularly useful for analyzing complex mixing problems where there are many more sources compared to isotope systems. Source apportionment of atmospheric Pb over a region requires consideration of isotopic compositions of multiple endmembers in which the Pb isotopic

composition of each endmember may be spread over a significantly large range. Thus, it is preferable to apply robust Bayesian models such as MixSIAR to these kinds of data set where we can consider multiple endmembers along with their uncertainty for determination of the proportion of contribution by the sources.

The means and 1SDs of $^{206}Pb/^{207}Pb$, $^{208}Pb/^{207}Pb$ and $^{208}Pb/^{206}Pb$ of the sources, and the isotopic composition of the aerosols were fed to the model framework in R (Stock et al., 2018). Due to limited number of source data in literature, with respect to ^{204}Pb, the comprehensive modelling was always conducted using ^{206}Pb, ^{207}Pb, and ^{208}Pb isotopes. With inadequate data, the standard deviations may not accurately represent the true heterogeneity in sources. Consequently, it can compromise the accuracy and reliability of MixSIAR results by generating higher uncertainties in source contributions and ambiguous source identifications. However, as the ratios relative to ^{204}Pb stem from distinct decay chains and possess the ability to discern source ages, the utilization of ^{204}Pb contributes to improved source apportionment accuracy (Baron et al., 2014; Longman et al., 2018). Thus, in order to validate the reliability of the modelling, results derived from ^{206}Pb, ^{207}Pb and ^{208}Pb isotopes, the aerosol mixture from Singapore for the last decade and its potential end members were subjected to MixSIAR analysis specifically considering the ^{204}Pb isotope as well. While compiling the source data from literature and this study, the values that were greater/less than 2SD of the mean were treated as outliers and eliminated. This reduces the overlapping of sources and increases model accuracy (Longman et al., 2022). The large mixture datasets the mixture Pb isotope ratios were combined every 5‰ with respect to $^{206}Pb/^{207}Pb$ ratios. The model was run using 3 parallel chains with a "long" MCMC chain length of 300,000 iterations. To ensure that the chains reached equilibrium, the first 200,000 iterated values were discarded/“burned”. The remaining samples were “thinned” by keeping every 100th iterated value (Stock and Semmens, 2016). The model convergence was checked using Gelman Rubin diagnostics.

This model can be executed in both concentration-dependent and concentration-independent versions. Concentration-dependent stable isotope mixing models are important in source apportionment studies, particularly when dealing with multiple sources having differences in elemental concentrations (Cox et al., 2023; Phillips and Koch, 2002). Accurate concentration data for the sources is a necessity for effectively utilizing concentration-dependent stable isotope mixing models. This accuracy can only be achieved when isotope and elemental concentration

data of the same sample set are available. While compiling data for India and SEA countries from the past decade such comprehensive concentration data for sources were not available. Hence the concentration-independent model was relied upon. However, to test the validity of the concentration-independent model, the concentration-dependent model was applied in case of Indian aerosol mixture. For rest of the objectives, as most of source data were analyzed in this study itself, the concentration-dependent model was utilized.

2.9.5. Quantification of Metal Emissions from Traffic Sources

The calculations for emissions of each metal were performed separately for EE, NEEs from internal combustion engines (ICEVs), and NEEs from EVs. Non-exhaust emission has been categorized into tire wear, brake wear and road abrasion. The two resultant NEE data from ICEVs and EVs were added to get the total NEE (ton/yr). The estimated metal concentrations were incorporated in the emission equations (Tian et al., 2015). The equations utilized for the calculations are as follows:

$$E_{ICEV} = EF_{ICEV} \times [X] \times M \times C \quad \text{..... 3.5}$$

Where, E_{ICEV} is the metal emitted in tons/year; EF_{ICEV} is the emission factor (g/km) for fuels when calculating EEs and for NEEs, EF_{ICEV} denotes the emission factors (g/km) for brake wear, tire wear, or road abrasions as applicable; [X] is the average concentration of the concerned element in mg/kg for vehicular exhaust, brake wear, tire wear or road abrasion as applicable; M is the average mileage in km/L and C is the fuel consumption of total car population in liter (L).

$$E_{EV} = EF_{EV} \times [X] \times M \times N_{EV} \quad \text{..... 3.6}$$

Where, E_{EV} is the metal emitted in tons/year; EF_{EV} is the emission factor (g/km) in EVs, for brake wear, tire wear, or road abrasions as applicable; [X] is the average concentration of the concerned element in mg/kg for brake wear, tire wear or road abrasion as applicable; M is the average mileage in km traveled by an EV in one full charge and N_{EV} is the population of EVs.

CHAPTER 3: RESULTS AND DISCUSSIONS

3.1. Sources of atmospheric Pb in India and South East Asian (SEA) countries in the last decade

South and Southeast Asia (SEA) have become a hotspot for anthropogenic PM emissions due to rapid industrialization, coal combustion, high-temperature industrial processes, vehicular traffic, and biomass burning (Ericson et al., 2021). Isotopes of Pb have proven invaluable for source apportionment, enabling the identification of multiple contributors, including legacy gasoline Pb, coal combustion, and high-temperature industrial activities.

In Singapore, the late phase-out of leaded gasoline in surrounding countries like Indonesia (2006) and Myanmar (2016) has left residual legacy Pb in the environment. Seasonal wind patterns play a significant role in transporting Pb-rich air masses from coal mines and industrial regions in Indonesia and China. Additionally, local sources like vehicular emissions and waste incinerators also contribute. Notably, Pb isotopic analysis of aerosols collected over a year in Singapore revealed distinct seasonal variations, with Northeast Monsoon winds carrying emissions from China and Vietnam, and Southwest Monsoon winds transporting pollutants from Indonesia (**Figure 1**).

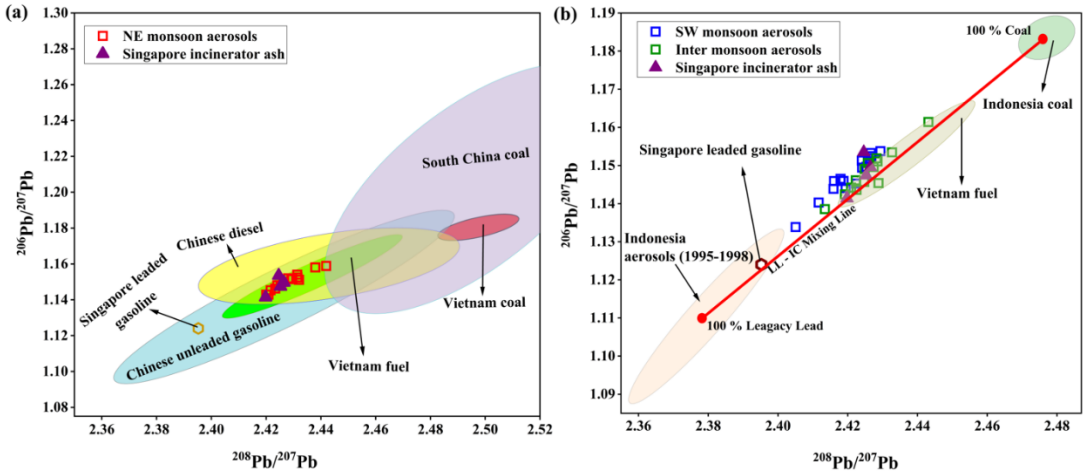

Figure 1: *Triple isotope plot of Pb for (a) NE and (b) SW & IM seasons with reference to different plausible end members. The mixing line between legacy lead (LL) and Indonesian coal (IC) is shown in red. References: Indonesian coal & aerosols and Vietnamese coal & fuel (Bollhöfer and Rosman, 2000; Díaz-Somoano et al., 2009 and Chifflet et al., 2018); Chinese diesel, unleaded gasoline and coal (Bi et al., 2017); Singapore leaded gasoline and incinerator ash (Carrasco et al., 2018).*

Elemental ratios of V/Pb and V/Ni indicated influence of coal combustion and ship emissions in South west and inter monsoon seasons. While, in North east monsoon, elemental ratio indicates that the metals were primarily sourced from traffic (Chifflet et al., 2018) and industrial emissions (**Figure 2**)

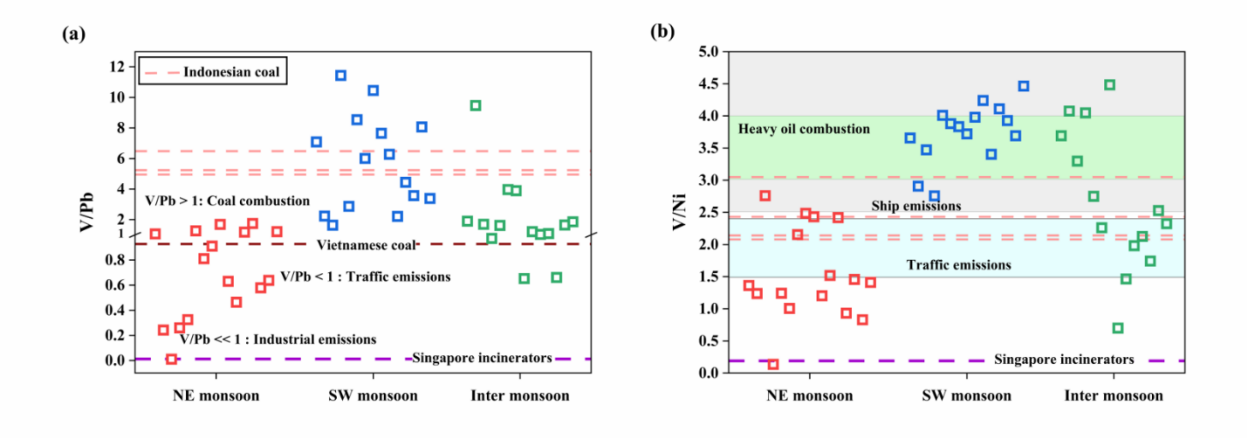

Figure 2: *Seasonal variations in (a) V/Pb and (b) V/Ni ratios in Singapore aerosols. Elemental ratios for Indonesian coal and Vietnamese coal have been adopted from Belkin et al. (2009) and Chifflet et al. (2018) respectively. V/Ni ratios for ship emissions were adopted from Wu and Huang (2021) and traffic emissions from Chifflet et al. (2018). Both the elemental ratios of Singapore incineration dust were adopted from Yin et al. (2008).*

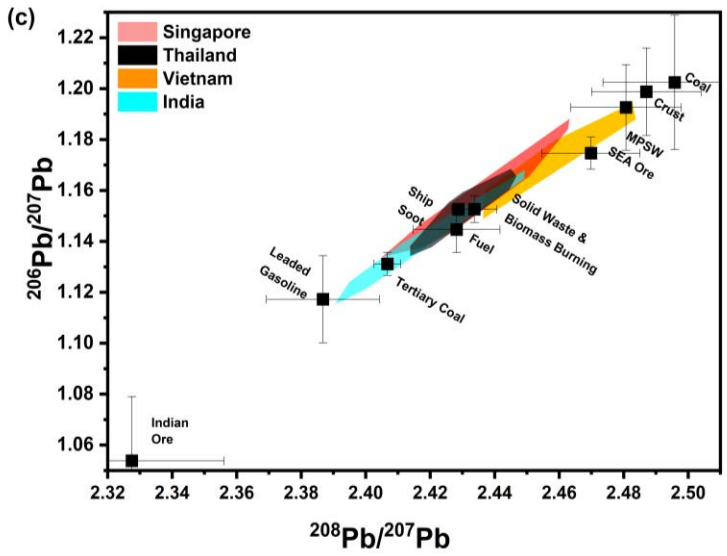

Figure 3: *Three – isotope plots of the aerosol mixtures from India, Singapore, Thailand, Vietnam and their sources from previous literatures in $^{208}Pb/^{207}Pb$ vs $^{206}Pb/^{207}Pb$ space*

The study further utilized a comprehensive dataset of Pb isotopic compositions (**Figure 3**) and elemental ratios from India and SEA countries (Singapore, Thailand and Vietnam) for the last decade (Carrasco et al., 2018; Chifflet et al., 2018; Das et al., 2023; Kayee et al., 2021, 2020; Ray et al., 2022) to perform source apportionment of atmospheric Pb. Findings indicate that coal combustion and industrial emissions, were the dominant sources of atmospheric Pb for India

in the last decade. However, for the SEA countries, the largest anthropogenic source was resuspension of leaded gasoline. Another significant finding was that ship emission is a significant contributor towards atmospheric Pb, although data on elemental concentrations and Pb isotopes of ship oil are scarce (**Figure 4**).

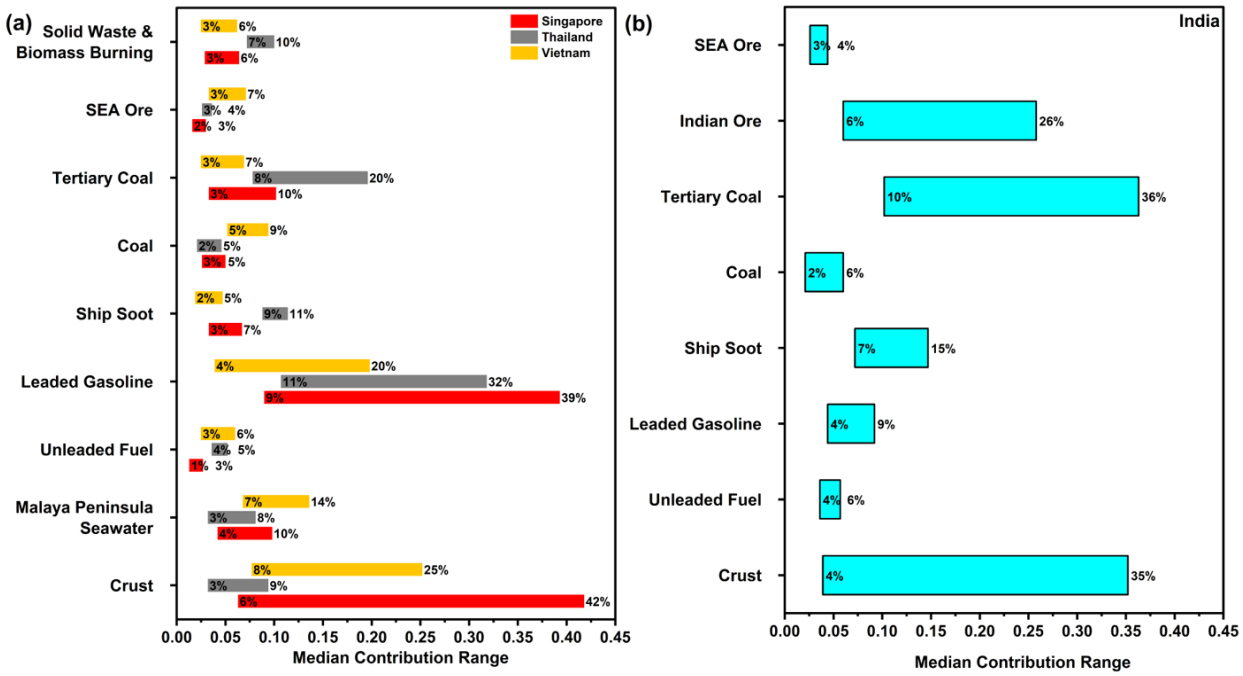

Figure 4: *Median contribution of individual sources towards atmospheric Pb in (a) SEA countries and (b) India determined from MixSIAR simulation. The percentages on left-hand side and right-hand side of the bars represents the minimum and maximum contributions from each source respectively.*

The persistence of legacy Pb, combined with modern anthropogenic emissions, underscores the complex interplay of sources contributing to atmospheric Pb pollution in South and Southeast Asia. Updated isotopic and elemental datasets are essential for accurately identifying sources and mitigating their impacts on public health and the environment.

3.2. Source apportionment and emission projections of heavy metals from traffic sources in India

Road traffic emissions are a major contributor to urban PM, arising from both exhaust emissions (EEs) and non-exhaust emissions (NEEs). While EEs originate from the incomplete combustion of fuel and lubricant volatilization, NEEs stem from abrasive sources such as brake wear, tire wear,

road surface abrasion, and the resuspension of road dust. Both emission types significantly contribute to urban atmospheric metal pollution, with toxic elements such as Ni, Cu, Zn, Pb etc posing severe health risks including respiratory and cardiovascular diseases (Cunha-Lopes et al., 2022; Demir et al., 2022; Harrison et al., 2012; Lopez et al., 2023; Zhang et al., 2020).

NEEs have gained attention due to their substantial contribution to PM, particularly in regions with heavy traffic. Tire wear, enriched in Zn due to its use in vulcanization processes, and brake wear, containing high levels of Cu, Ba, and Pb from frictional materials, are key sources of heavy metals in urban road dust (Budai and Clement, 2018; Grigoratos and Martini, 2015; Lin et al., 2015).

Despite efforts to promote electric vehicles (EVs), EEs remain a growing concern in India due to the increasing population of internal combustion engine vehicles (ICEVs). Projections indicate that India's vehicle fleet will quadruple by 2045, with ICEVs continuing to dominate. This trend suggests a corresponding increase in EEs. NEEs, on the other hand, will persist as a major source of atmospheric metals due to their association with both ICEVs and EVs (**Figure 5**).

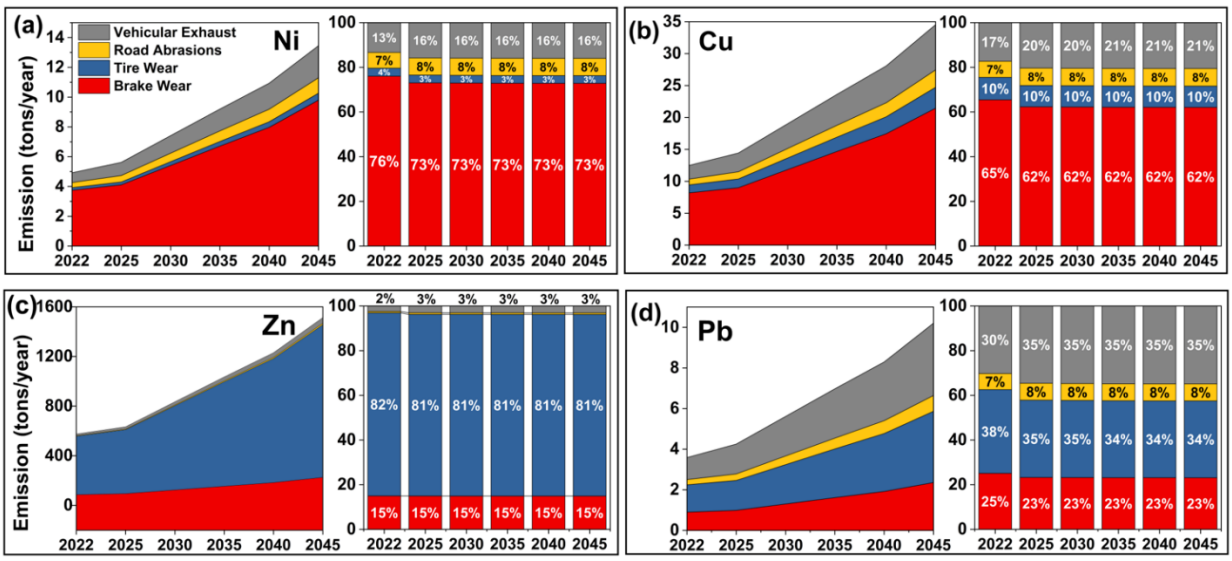

Figure 5: *Stacked area plots representing total emissions of vehicular exhaust, tire wear, brake wear and road abrasions in tons/year. The stacked bar plots depict the percentage contribution of each source towards total metal emissions from traffic sources for (a) Ni (b) Cu (c) Zn and (d) Pb in the years 2022, 2025, 2030, 2035, 2040 and 2045. About 60 % - 70 % of the emissions of Ni and Cu are from brake wears while the major source of Zn emission is tire wear particles. The NEE (tire wear, brake wear, road abrasions) sources contribute more towards Pb emission than EE sources*

The use of elemental ratios and Pb isotopic signatures (**Figure 6a and 6b**) enables the identification of these sources, highlighting the significant contributions of both EEs and NEEs to

urban road dust. Bayesian mixing models like MixSIAR estimate that road dust comprises approximately equal contributions from EE and NEE sources, with significant inputs from brake and tire wear (**Figure 6c**).

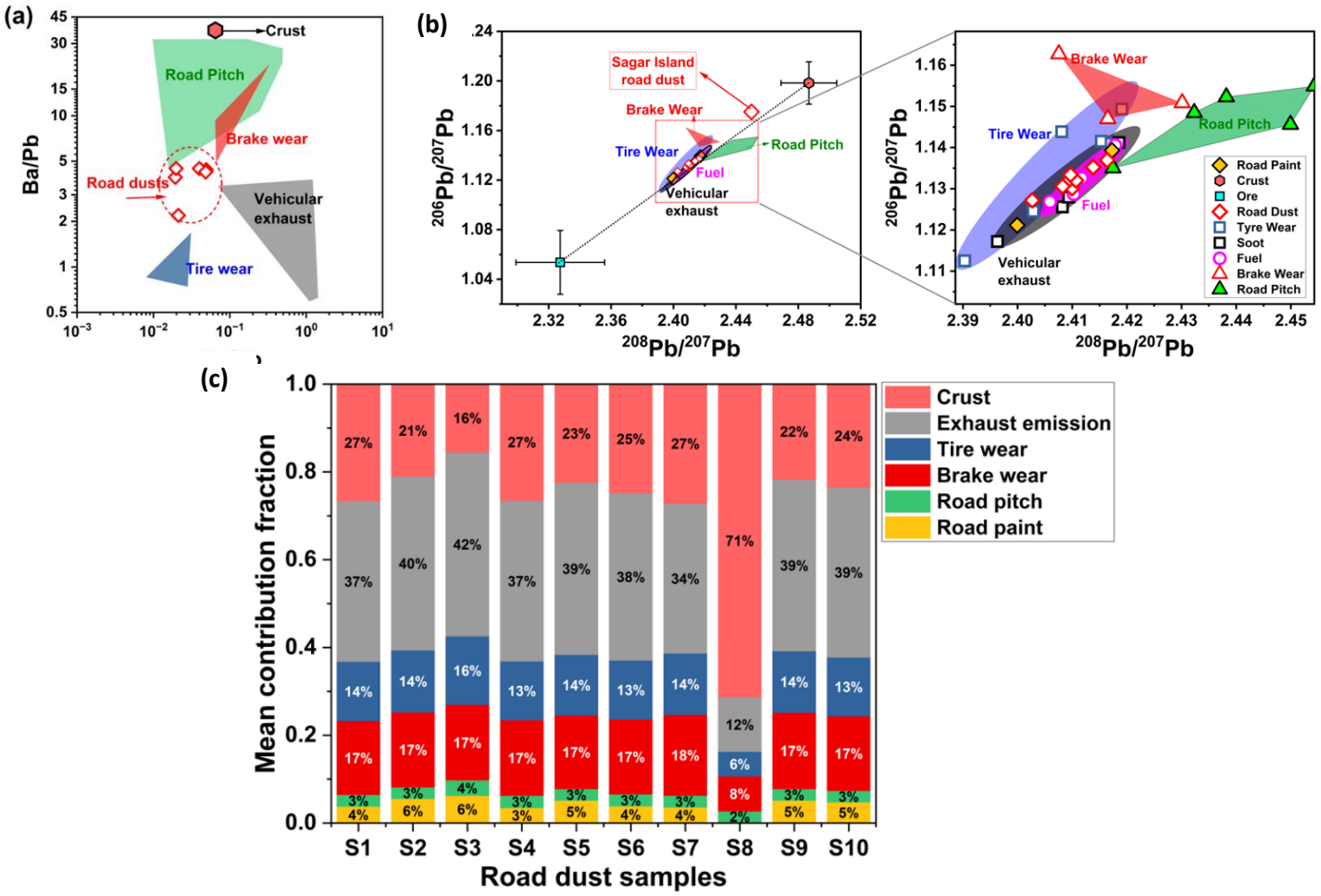

***Figure 6**: (a) Elemental ratios plotted as (a) bivariate plot of Mo/Pb vs Ba/Pb and (b) ternary plot of Pb/Mn, Cu/Zn and Fe/Al demonstrates that the characteristic ratios of road dusts lie between those of the EE and NEE sources. (b) Three-isotope plots of $^{208}Pb/^{207}Pb$ vs $^{206}Pb/^{207}Pb$ for Indian fuel, vehicular exhaust, road dusts, tire wear, brake wear, road pitch and road paint. The right-hand panel provides an enlarged view of the squared section from the left-hand panel. (c) MixSIAR results for mean contribution of Pb towards crust, exhaust emission, tire wear, brake wear, road pitch and road paint towards road dusts from eastern India. All the samples demonstrate consistent contributions from the sources except sample "S8", from Sagar island, a pristine location having heavy influence from natural crust*

3.3. Sources of atmospheric Pb in and around a coal-fired power plant in India

This study investigates the sources of atmospheric Pb in $PM_{2.5}$ aerosols around the Neyveli Lignite Corporation India Limited (NLCIL), a major lignite-fired power plant in southern India. Elemental concentrations and Pb isotopic compositions were analyzed to trace the origins of Pb and assess the relative contributions of natural and anthropogenic sources.

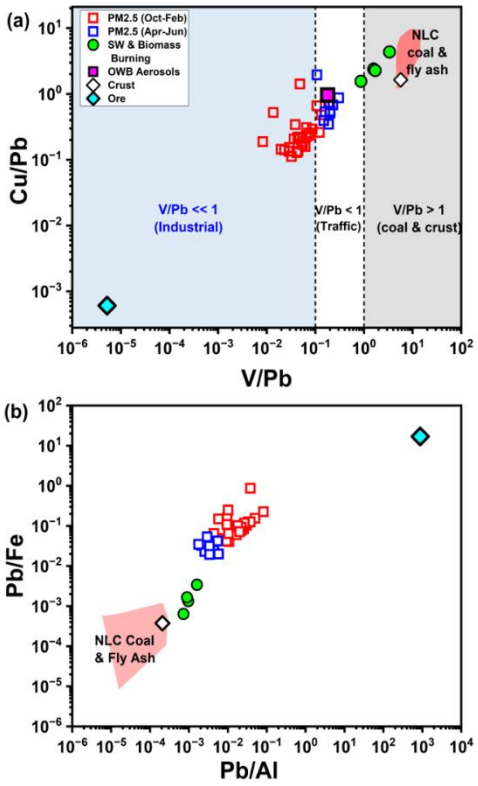

Figure 7: *Elemental ratios plotted as (a) V/Pb vs Cu/Pb (b) Pb/Al vs Pb/Fe indicate that the $PM_{2.5}$ aerosols are a mixture of crust, coal & fly ash, solid waste & biomass burning and industrial smelting (depicted as ore in the figure). The characteristic V/Pb ratios for industrial, traffic and coal/crustal sources (Das et al., 2018) are marked as shaded regions for reference. The October-February aerosols have V/Pb<<1 and hence plot in the region of industrial emissions. The open waste burning aerosols from Delhi's Okhla landfill site (Kumar et al., 2018) overlapping with April-June aerosols is plotted in V/Pb vs Cu/Pb space for reference. The April-June aerosols seem to be more influenced by solid waste & biomass burning and crustal sources with decreased Pb/Fe and Pb/Al ratios than the October-February aerosols. The elemental concentration data for crust has been adopted from Rudnick and Gao 2003.*

Contrary to observations from the last decade, the elemental ratios (**Figure 7**) and Pb isotopic signatures (**Figure 8a**) indicate that Pb and other heavy metals in $PM_{2.5}$ aerosols are not primarily sourced from coal combustion in the study region. Instead, the MixSIAR results reveal significant contributions from open burning of biomass and solid waste (**Figure 8b**). This finding is supported by the distinct Pb isotopic ratios in the aerosols, which differ substantially from those of local lignite and associated fly ash. The aerosols display isotopic compositions that align more closely with solid waste burning, crustal dust, and, to a lesser extent, legacy Pb from historical use of leaded gasoline.

Seasonal variations were observed in Pb sources. During summer (April–June), aerosols exhibited lower enrichment factors for Pb and isotopic signatures indicative of a greater crustal influence, likely due to increased soil resuspension from local fires.

The findings indicates that stricter regulations put forth in 2015 by India are being effective in controlling metal emissions from coal combustion. However, stringent

regulations should be implemented to stop uncontrolled emission from open burning of biomass and solid wastes.

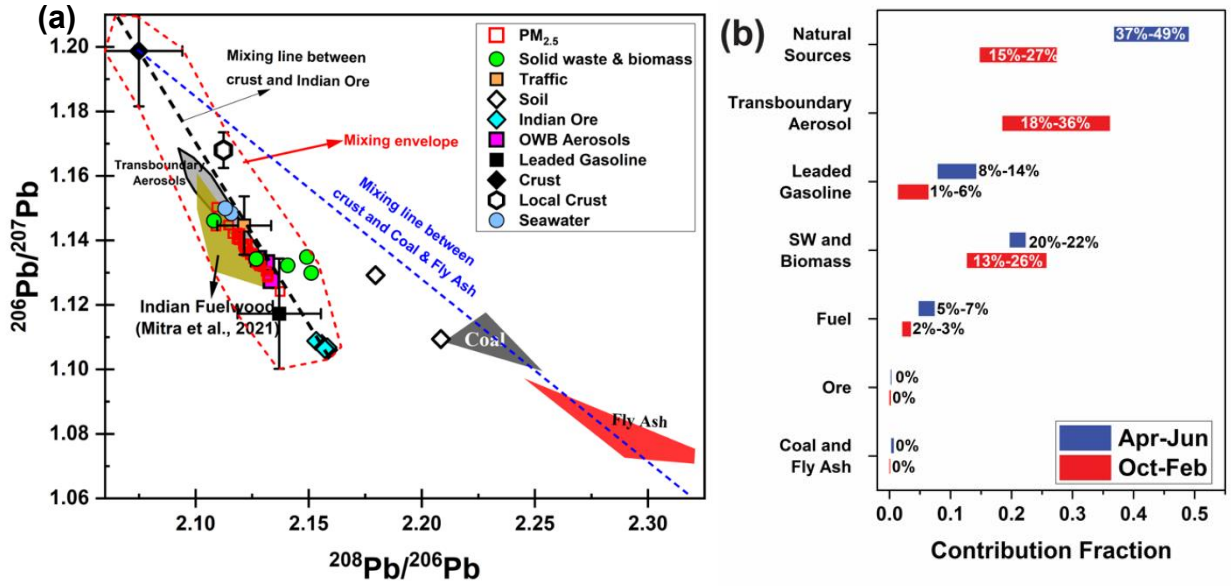

***Figure 8**: (a) The Pb isotopic compositions of the $PM_{2.5}$ aerosols and relevant end members illustrated in three-isotope space ($^{208}Pb/^{206}Pb$ vs $^{206}Pb/^{207}Pb$).(b) Median contribution of individual sources towards atmospheric Pb determined from MixSIAR simulation. The percentages over/beside the bars represent the range of contributions from each source.*

3.4. Tracing atmospheric Pb sources in India's pristine region: a case study from the Andaman and Nicobar Islands

This study investigates the sources of atmospheric Pb in PM_{10} and $PM_{2.5}$ aerosols in the Andaman and Nicobar (A&N) Islands, a pristine environment with minimal industrial and coal combustion activities, which were the primary sources of atmospheric Pb in the last decade. Using elemental concentrations and Pb isotopic ratios, the study reveals distinct seasonal variations in Pb sources. During the winter, transboundary aerosols from SEA, particularly from Thailand, emerge as significant contributor, evidenced by overlap in isotopic signatures with SEA aerosols (**Figure 9**). In contrast, the monsoon season is dominated by local sources, that include vehicular and ship emissions, crustal resuspension. Stronger marine influence was observed in monsoon than in winter with higher Na/Mg ratios in coarser PM_{10} particles.

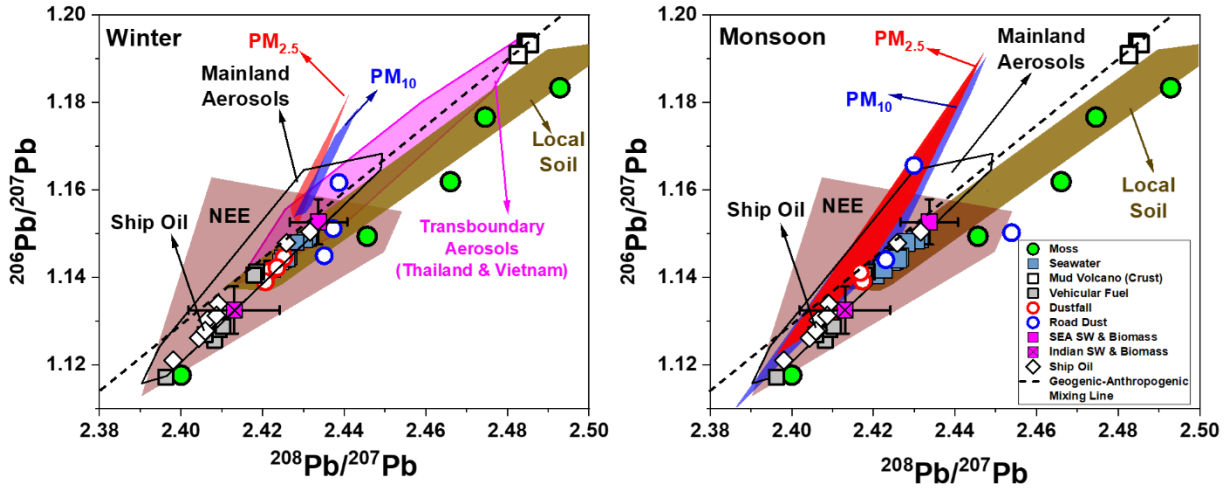

Figure 9: *Three isotope plots illustrating the Pb isotopic composition of aerosols as well as their potential sources in (a) winter and (b) monsoon seasons*

Remarkably, the Pb isotopic composition of the aerosols diverges from conventional geogenic-anthropogenic mixing lines, pointing to the presence of unique local sources which is highly urogenic and simultaneously less thorogenic contrary to most geogenic and anthropogenic samples, which demonstrate high thorogenic and urogenic signatures simultaneously. The end member explaining such a Pb isotopic composition was found out to be emissions from bullets and missiles utilized for military activities, as it is a military zone (Andaman & Nicobar Command, 2022; PIB, 2023; Prakash, 2003; PTI, 2023) (**Figure 10**).

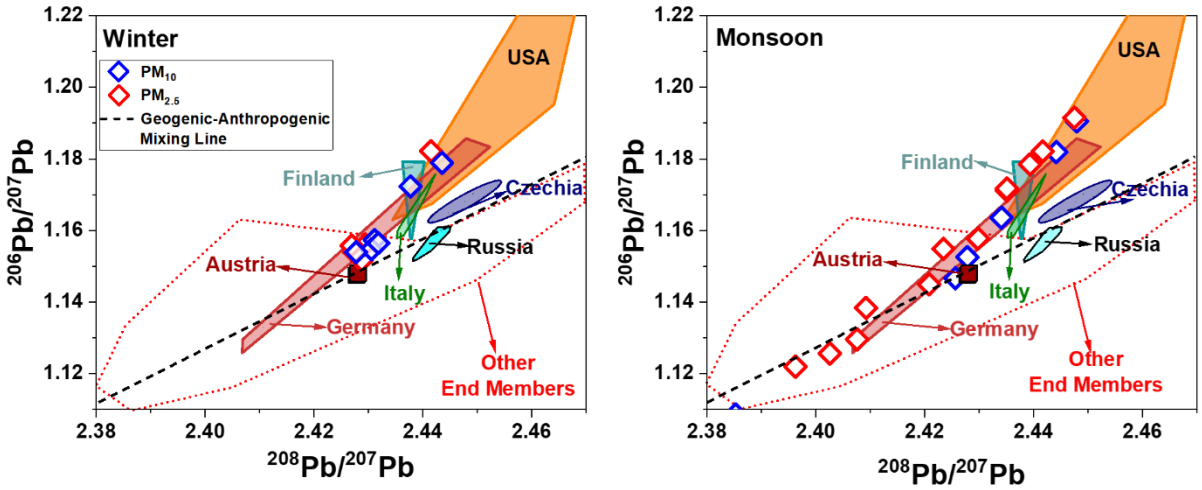

Figure 10: *Three isotope plots illustrating the Pb isotopic composition of aerosols, the conventional end members as well as bullets from different regions in (a) winter and (b) monsoon seasons*

Bullets account for up to 23% of Pb during the monsoon and 18% in winter, indicating consistent contributions year-round (**Figure 11**). These findings underscore the significant role of localized anthropogenic emissions, including shipping, vehicular activity, and military operations, in influencing atmospheric Pb levels in environments devoid of other major anthropogenic sources.

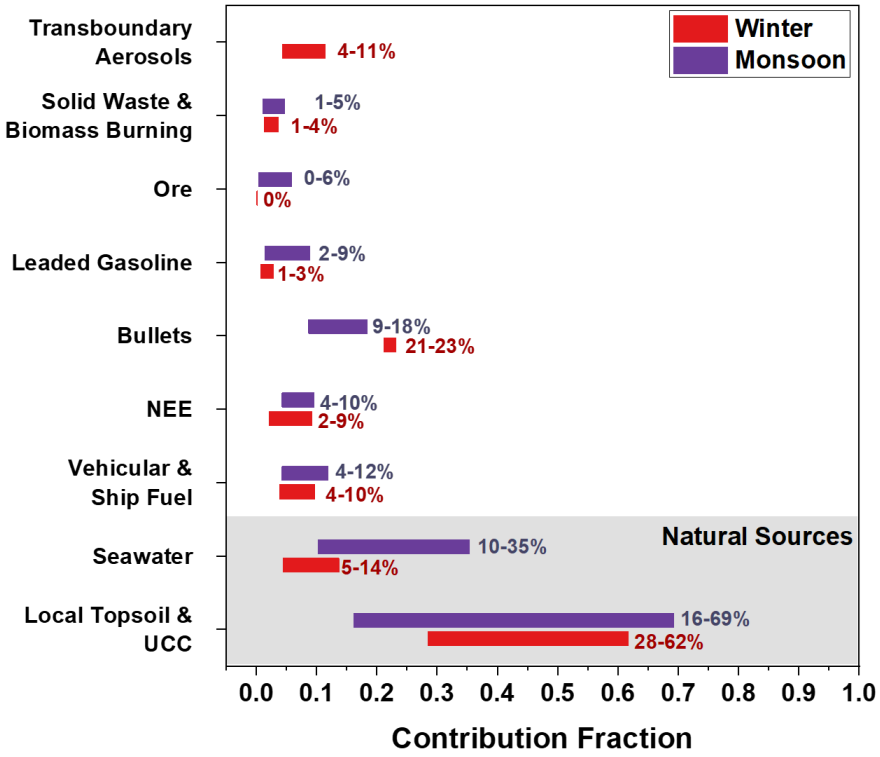

Figure 11: *Contribution of different sources towards atmospheric Pb in A & N Islands as quantified using MixSIAR*

3.4. Remediation of atmospheric Pb

This study explores the potential of ferns, as natural mitigators of atmospheric Pb pollution in densely populated urban settings with high PM pollution. Sampling was conducted in Kolkata and Howrah, two of the most polluted cities in eastern India, where the fern species, *Pteris vittata* and *Pteridium aquilinum* were found to grow abundantly (Gupta et al., 2008; Upadhyay et al., 2014). The research utilized gravimetric techniques, surface characterization (SEM-EDX), elemental concentration analyses, and Pb isotopic composition to evaluate the foliar dust capture capacity of ferns and their ability to assimilate anthropogenic Pb from PM10 aerosols and dustfall (DF).

The findings reveal that ferns exhibit a high dust capture efficiency, with loose dust (LD) and wax-bound dust (WD) loads exceeding previously reported values from urban and industrial regions.

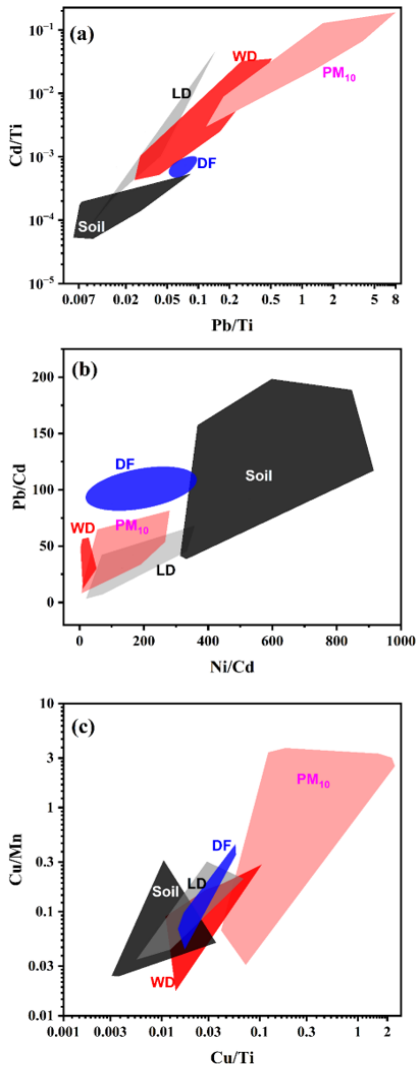

Figure 12: *Elemental ratios plotted as (a) Pb/Ti vs Cd/Ti (b) Ni/Cd vs Pb/Cd and (c) Cu/Ti vs Cu/Mn. Pb/Ti vs Cd/Ti demonstrates that the characteristic ratios of LDs and WDs lie between those of soil, PDs and PM_{10}, with some of WDs overlapping with PM10 aerosols. Thus, the leaf surface dusts were a mixture of soil, PD and PM10. Overlapping of LD and WD with PM10 aerosols in Ni/Cd vs Pb/Cd suggests that these elements in the leaf surface dusts were primarily sourced from the atmosphere. Cu/Ti vs Cu/Mn suggests that these elements were primarily of crustal origin.*

Elemental concentrations (**Figure 12**) and Pb isotopic analyses (**Figure 13**) demonstrate that Pb in fern tissues originates primarily from atmospheric fallouts, including PM_{10} and dust fall, with minimal influence from soil-derived geogenic sources.

Pb isotopic ratios indicate that bioavailable fractions of Pb in soil, associated with exchangeable, carbonate, and reducible phases, which have similar isotopic compositions as that of dustfall (DF) are preferentially absorbed by fern roots, rather than the isotopically distinguishable silicate fraction (**Figure 14**). The MixSIAR model quantified that 53–73% of Pb in fern leaves and 33–86% in roots originates from atmospheric sources (**Figure 15**).

Using this foliar metal concentration data and indoor PM_{10} concentrations from previous publications, it was estimated that a 1 m^2 fern cover could remain effective for several days in capturing Cr, Ni, Cu, and Pb in a 10 m^2 residential room. These results highlight the suitability of *Pteris vittata* and *Pteridium aquilinum* for indoor air remediation, highlighting their high metal tolerance, dust capture efficiency, and adaptability to varied environmental conditions.

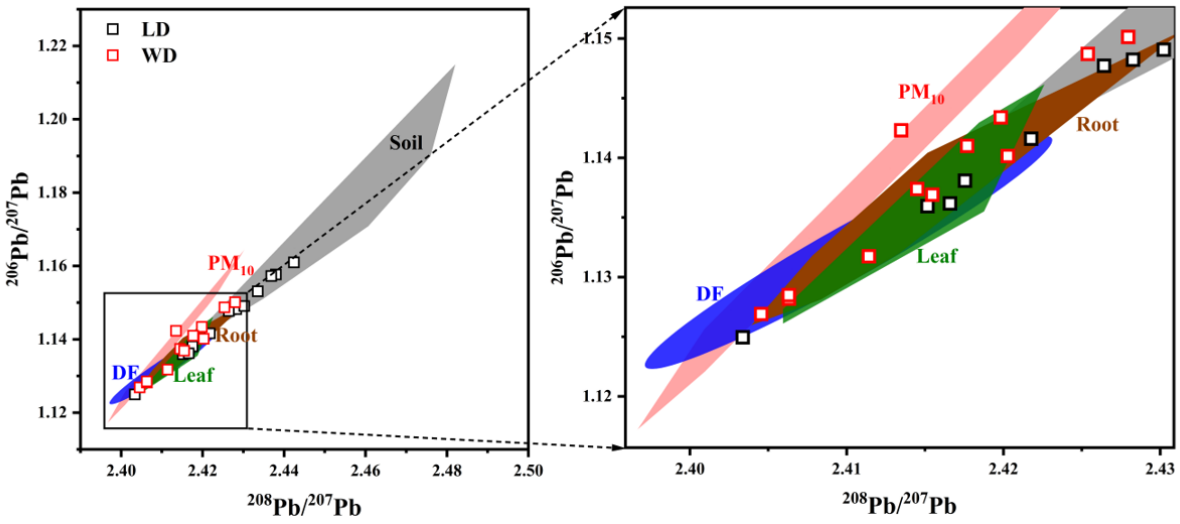

Figure 13: *Triple isotope plots of $^{208}Pb/^{207}Pb$ vs $^{206}Pb/^{207}Pb$ for PM_{10} aerosols, DF, LD, WD, leaf, root and soil. The soil, PM10, DF, leaf and roots are depicted as fields in grey, light red, blue, green and brown colours. The open black and red squares represent LD and WD respectively. The triple isotope plots demonstrate that the sources of Pb in WD, roots and leaves are primarily a mixture of PM_{10} and DFs, while LD demonstrates partial influence from soil along with PM_{10} and DF.*

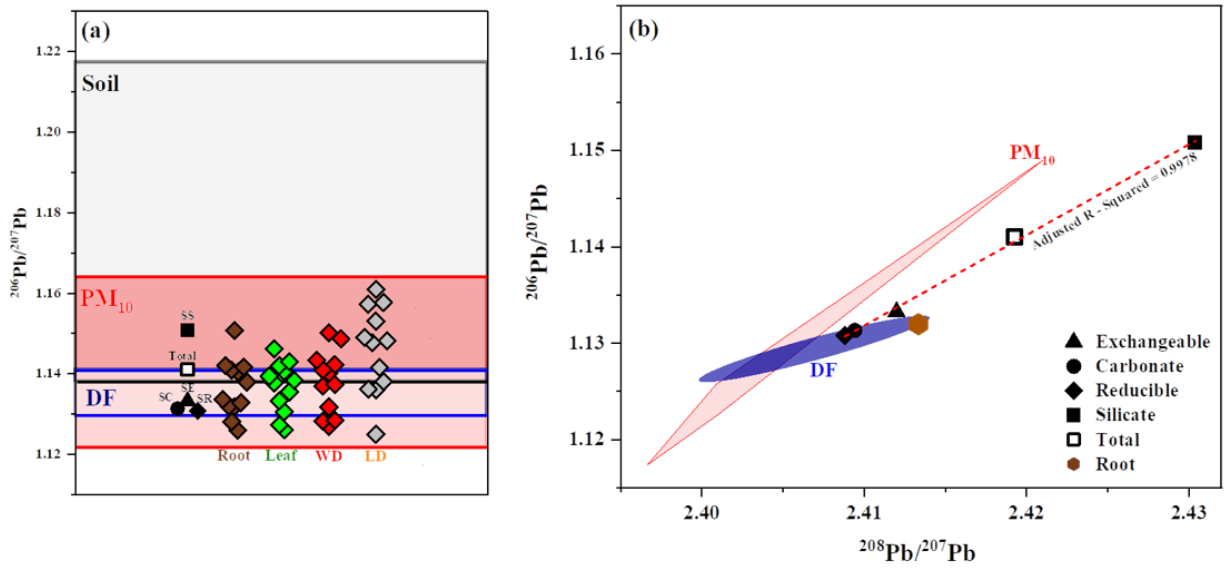

Figure 14: *(a) $^{206}Pb/^{207}Pb$ composition of soil, PM10, DF, root, leaf, WD and LD. SE, SC, SR and SS are exchangeable, carbonate, reducible and silicate fraction of soil respectively. LDs showed a higher $^{206}Pb/^{207}Pb$ signature compared to WDs, indicating the contribution of Pb from regional soil in LD. Conversely, WDs displayed a stronger association with PM_{10}. Isotopic composition of root is comparable to SE, SC and SR, which in turn are similar to DF. (b) Triple isotope plots of $^{208}Pb/^{207}Pb$ vs $^{206}Pb/^{207}Pb$ for the exchangeable (SE), carbonate (SC), reducible (SR), silicate (SS) fractions of the sequentially leached soil samples. The mixing line between SR and SS are plotted as red dashed line. The Pb isotopic compositions for corresponding root sample and atmospheric fallout samples (DF and PM_0) compositions are plotted for comparison*

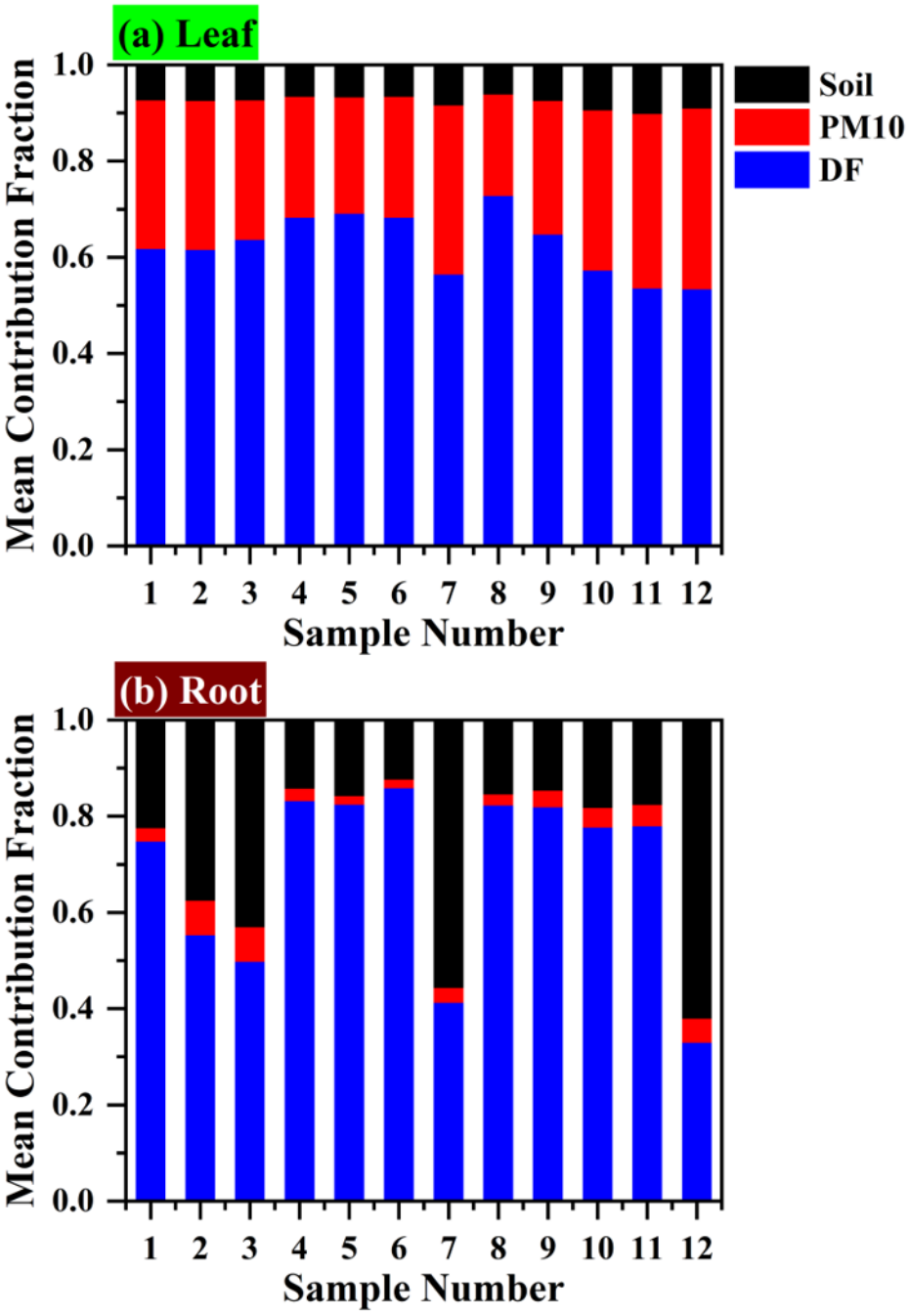

Figure 15: *MixSIAR results for mean contribution of soil, DF and PM^{10} aerosols towards (a) leaf and (b) root Pb of the fern samples. The dominant sources of Pb in leaves were DF and PM10 aerosols, whereas Pb within fern roots primarily originated from soil and DF*

CHAPTER 3: CONCLUSIONS

This thesis provides a comprehensive investigation into the sources of atmospheric lead (Pb) pollution across urban, industrial, and pristine environments. Through advanced elemental and Pb isotopic composition analyses, this work has identified the dominant sources of Pb, examined the seasonal variations in its concentration, and explored the potential of innovative remediation strategies.

Starting with a detailed source apportionment of Pb emissions over the last decade, this study investigates whether there are unrecognized and underdetermined sources of atmospheric Pb in India as well as in SEA countries.

In the last decade, Pb resuspension from legacy leaded gasoline persists as a significant source, particularly in SEA. Despite its phaseout over two decades ago, its influence remains prominent in SEA and, to a lesser extent, in India. In addition to this ship emissions, which is not a much analyzed source so far were identified as a consistent and significant source of Pb, reflecting the presence of heavy metals in heavy fuel oils and other marine fuels and oils.

In India, while industrial emissions and coal combustion dominated Pb sources in the last decade, stricter environmental regulations and the implementation of cleaner technologies have markedly reduced their contribution. This is evident from coal-fired power plants, where most Pb and other heavy metals in PM are derived from other anthropogenic activities rather than from coal. Interestingly, open burning of biomass and solid waste was identified as a major contributor to Pb emissions in regions of coal combustion. The pervasive issue of open biomass and solid waste burning in coal combustion-dominated regions emerges as a critical source of atmospheric Pb.

This practice, often unregulated, contributes significantly to the heavy metal burden in the air. Addressing this issue requires the implementation of stricter waste management policies, the promotion of community-level awareness campaigns, and the enforcement of alternative, sustainable waste disposal methods. Immediate and coordinated efforts to eliminate open burning practices are essential to mitigate its adverse impacts and to foster healthier, cleaner environments in these regions.

Other than the conventionally recognized anthropogenic sources of atmospheric Pb such as coal and industrial emissions, the role of NEE in urban road pollution, was underexplored. Although EE have been studied, NEE, primarily originating from tire and brake wear, as well as road surface abrasions represents a significant component of traffic-related pollution as observed from this study. It was detected that NEE contributes almost as much Pb and other metals towards urban road dusts as EE. Emission projections indicate that even with increased EV adoption by 2045, the dominance of ICEVs in India's vehicular fleet will continue to shape the emission profile. Consequently, traffic-related Pb emissions are expected to remain largely unchanged, necessitating additional measures to address urban pollution.

Source apportionment studies in remote, pristine setting highlights how underexplored and otherwise undetectable sources become visible in the absence of larger pollution sources. In the Andaman and Nicobar Islands, where industrial and coal combustion activities are absent, the study revealed that anthropogenic sources like military activities and ship emissions are the dominant contributors to atmospheric Pb. Emissions related to military activities as determined with bullets as a proxy, emerged as a significant and previously unrecognized Pb source, while ship emissions consistently influenced Pb levels year-round. Seasonal variations with reversal in wind patterns demonstrate that seawater contributions peaking during the monsoon, with crustal and natural inputs remaining stable year-round.

Natural sources have always been dominant contributors to atmospheric Pb levels globally, a trend that persists in the findings of this study. Dust storms, soil erosion, and agricultural activities can release these materials into the atmosphere, particularly in arid and semi-arid regions. This contribution is not only localized but can also extend across continents, as observed in transcontinental dust transport events. Sea spray aerosols are another critical natural source, particularly in coastal and marine regions. The interaction between wind, waves, and seawater generates aerosols that carry marine-derived trace metals, including Pb. Seasonal variations, such as those observed during monsoon and storm seasons, can amplify this contribution, making sea spray a variable but significant factor in atmospheric Pb levels.

Building upon the understanding of natural and anthropogenic sources of atmospheric Pb, innovative remediation strategies were explored, focusing on the potential of ferns as effective biofilters for Pb capture. This approach leverages the natural metal tolerance and air-purifying

capabilities of perennial fern species, which are well-suited to tropical climates and a variety of environmental conditions. These plants have shown remarkable efficiency in capturing Pb and other heavy metals from indoor air, presenting an accessible and environmentally sustainable solution for mitigating metal exposure in urban environments.

Investigations revealed that the roots of the ferns along with the leaves also play a crucial role in metal uptake. When integrated into an active filtration system, where PM is also captured by the substrate where the fern roots grow, the overall efficiency of the system is enhanced as PM is captured by leaves, roots and the substrate.

However, the disposal of metal-laden fern leaves presents a challenge, as improper management could lead to secondary pollution. To mitigate this, safe disposal strategies, such as converting contaminated biomass into eco-friendly products like unfired earth bricks, are essential to prevent further environmental harm. Overall, fern-based biofiltration presents a promising, sustainable solution for reducing indoor metal pollution and enhancing urban air quality.

By identifying both conventional and previously overlooked sources, as well as exploring innovative solutions like fern-based biofiltration, this research provides a comprehensive framework for addressing Pb pollution. Thus, it is essential to implement stricter regulations, promote awareness, and adopt sustainable remediation practices to effectively mitigate the impact of Pb on human health and the environment.

REFERENCES

Andaman & Nicobar Command, 2022. Routine Firing Exercise from Netaji Subhash Chandra Bose Island (Ross Island). Army and Navy Components #ANC carried out a seaward joint firing drill aimed at honing interoperability. Together we are stronger #Victorythroughjointness #Alwaysbattleready https://t.co/3pLggaGCjY. Twitter.

Baker, J., Peate, D., Waight, T., Meyzen, C., 2004. Pb isotopic analysis of standards and samples using a 207Pb–204Pb double spike and thallium to correct for mass bias with a double-focusing MC-ICP-MS. Chem. Geol. 211, 275–303. https://doi.org/10.1016/j.chemgeo.2004.06.030

Baron, S., Tămaş, C.G., Le Carlier, C., 2014. How Mineralogy and Geochemistry Can Improve the Significance of Pb Isotopes in Metal Provenance Studies. Archaeometry 56, 665–680. https://doi.org/10.1111/arcm.12037

Bhuvaneshwari, S., Hettiarachchi, H., Meegoda, J.N., 2019. Crop Residue Burning in India: Policy Challenges and Potential Solutions. Int. J. Environ. Res. Public. Health 16, 832. https://doi.org/10.3390/ijerph16050832

Bollhöfer, A., Rosman, K.J.R., 2001. Isotopic source signatures for atmospheric lead: the Northern Hemisphere. Geochim. Cosmochim. Acta 65, 1727–1740. https://doi.org/10.1016/S0016-7037(00)00630-X

Budai, P., Clement, A., 2018. Spatial distribution patterns of four traffic-emitted heavy metals in urban road dust and the resuspension of brake-emitted particles: Findings of a field study. Transp. Res. Part Transp. Environ. 62, 179–185. https://doi.org/10.1016/j.trd.2018.02.014

Carrasco, G., Chen, M., Boyle, E.A., Tanzil, J., Zhou, K., Goodkin, N.F., 2018. An update of the Pb isotope inventory in post leaded-petrol Singapore environments. Environ. Pollut. 233, 925–932. https://doi.org/10.1016/j.envpol.2017.09.025

Chatterjee, D., McDuffie, E.E., Smith, S.J., Bindle, L., van Donkelaar, A., Hammer, M.S., Venkataraman, C., Brauer, M., Martin, R.V., 2023. Source Contributions to Fine Particulate Matter and Attributable Mortality in India and the Surrounding Region. Environ. Sci. Technol. 57, 10263–10275. https://doi.org/10.1021/acs.est.2c07641

Chifflet, S., Amouroux, D., Bérail, S., Barre, J., Van, T.C., Baltrons, O., Brune, J., Dufour, A., Guinot, B., Mari, X., 2018. Origins and discrimination between local and regional atmospheric pollution in Haiphong (Vietnam), based on metal(loid) concentrations and lead isotopic ratios in PM10. Environ. Sci. Pollut. Res. Int. 25, 26653–26668. https://doi.org/10.1007/s11356-018-2722-7

Corton, C.L., 2021. London Fog as Food: From Pabulum to Poison, in: Fuller, D., Saunders, C., Macnaughton, J. (Eds.), The Life of Breath in Literature, Culture and Medicine: Classical to Contemporary. Springer International Publishing, Cham, pp. 325–343. https://doi.org/10.1007/978-3-030-74443-4_16

Cox, T., Laceby, J.P., Roth, T., Alewell, C., 2023. Less is more? A novel method for identifying and evaluating non-informative tracers in sediment source mixing models. J. Soils Sediments 23, 3241–3261. https://doi.org/10.1007/s11368-023-03573-0

Cunha-Lopes, I., Alves, C.A., Casotti Rienda, I., Faria, T., Lucarelli, F., Querol, X., Amato, F., Almeida, S.M., 2022. Characterisation of non-exhaust emissions from road traffic in Lisbon. Atmos. Environ. 286, 119221. https://doi.org/10.1016/j.atmosenv.2022.119221

Das, R., Bin Mohamed Mohtar, A.T., Rakshit, D., Shome, D., Wang, X., 2018. Sources of atmospheric lead (Pb) in and around an Indian megacity. Atmos. Environ. 193, 57–65. https://doi.org/10.1016/j.atmosenv.2018.08.062

Das, R., Wang, X., Khezri, B., Webster, R.D., Itoh, M., Shiodera, S., Bin Mohamed Mohtar, A.T., Kuwata, M., 2023. Suspension of Crustal Materials from Wildfire in Indonesia as Revealed by Pb Isotope Analysis. ACS Earth Space Chem. 7, 379–387. https://doi.org/10.1021/acsearthspacechem.2c00270

Demir, T., Karakaş, D., Yenisoy-Karakaş, S., 2022. Source identification of exhaust and non-exhaust traffic emissions through the elemental carbon fractions and Positive Matrix Factorization method. Environ. Res. 204, 112399. https://doi.org/10.1016/j.envres.2021.112399

Díaz-Somoano, M., Kylander, M.E., López-Antón, M.A., Suárez-Ruiz, I., Martínez-Tarazona, M.R., Ferrat, M., Kober, B., Weiss, D.J., 2009. Stable Lead Isotope Compositions In Selected Coals From Around The World And Implications For Present Day Aerosol Source Tracing. Environ. Sci. Technol. 43, 1078–1085. https://doi.org/10.1021/es801818r

Draxler, R., 1998. An Overview of the HYSPLIT_4 Modelling System for Trajectories, Dispersion, and Deposition.

Dzierżanowski, K., Popek, R., Gawrońska, H., Sæbø, A., Gawroński, S.W., 2011. Deposition of Particulate Matter of Different Size Fractions on Leaf Surfaces and in Waxes of Urban Forest Species. Int. J. Phytoremediation 13, 1037–1046. https://doi.org/10.1080/15226514.2011.552929

Ericson, B., Hu, H., Nash, E., Ferraro, G., Sinitsky, J., Taylor, M.P., 2021. Blood lead levels in low-income and middle-income countries: a systematic review. Lancet Planet. Health 5, e145–e153. https://doi.org/10.1016/S2542-5196(20)30278-3

Fowler, D., Brimblecombe, P., Burrows, J., Heal, M.R., Grennfelt, P., Stevenson, D.S., Jowett, A., Nemitz, E., Coyle, M., Liu, X., Chang, Y., Fuller, G.W., Sutton, M.A., Klimont, Z., Unsworth, M.H., Vieno, M., 2020. A chronology of global air quality. Philos. Trans. R. Soc. Math. Phys. Eng. Sci. 378, 20190314. https://doi.org/10.1098/rsta.2019.0314

Gelwicks, J.T., Hayes, J.M., 1990. Carbon-isotopic analysis of dissolved acetate. Anal. Chem. 62, 535–539. https://doi.org/10.1021/ac00204a021

Grigoratos, T., Martini, G., 2015. Brake wear particle emissions: a review. Environ. Sci. Pollut. Res. 22, 2491–2504. https://doi.org/10.1007/s11356-014-3696-8

Guevara, M., 2016. Emissions of Primary Particulate Matter.

Gulson, B.L., Davis, J.J., Mizon, K.J., Korsch, M.J., Bawden-Smith, J., 1995. Sources of lead in soil and dust and the use of dust fallout as a sampling medium. Sci. Total Environ. 166, 245–262. https://doi.org/10.1016/0048-9697(95)04505-U

Gupta, A.K., Karar, K., Ayoob, S., John, K., 2008. Spatio-temporal characteristics of gaseous and particulate pollutants in an urban region of Kolkata, India. Atmospheric Res. 87, 103–115. https://doi.org/10.1016/j.atmosres.2007.07.008

Harrison, R.M., Jones, A.M., Gietl, J., Yin, J., Green, D.C., 2012. Estimation of the Contributions of Brake Dust, Tire Wear, and Resuspension to Nonexhaust Traffic Particles Derived from Atmospheric Measurements. Environ. Sci. Technol. 46, 6523–6529. https://doi.org/10.1021/es300894r

Hippocrates, 400AD. The Internet Classics Archive | On Airs, Waters, and Places by Hippocrates [WWW Document]. URL https://classics.mit.edu/Hippocrates/airwatpl.1.1.html (accessed 1.8.25).

Jeong, H., Ryu, J.-S., Ra, K., 2022. Characteristics of potentially toxic elements and multi-isotope signatures (Cu, Zn, Pb) in non-exhaust traffic emission sources. Environ. Pollut. 292, 118339. https://doi.org/10.1016/j.envpol.2021.118339

Kayee, J., Bureekul, S., Sompongchaiyakul, P., Wang, X., Das, R., 2021. Sources of atmospheric lead (Pb) after quarter century of phasing out of leaded gasoline in Bangkok, Thailand. Atmos. Environ. 253, 118355. https://doi.org/10.1016/j.atmosenv.2021.118355

Kayee, J., Sompongchaiyakul, P., Sanwlani, N., Bureekul, S., Wang, X., Das, R., 2020. Metal Concentrations and Source Apportionment of $PM_{2.5}$ in Chiang Rai and Bangkok, Thailand during a Biomass Burning Season. ACS Earth Space Chem. 4, 1213–1226. https://doi.org/10.1021/acsearthspacechem.0c00140

Komárek, M., Ettler, V., Chrastný, V., Mihaljevič, M., 2008. Lead isotopes in environmental sciences: A review. Environ. Int. 34, 562–577. https://doi.org/10.1016/j.envint.2007.10.005

Kumar, S., Aggarwal, S.G., Malherbe, J., Barre, J.P.G., Berail, S., Gupta, P.K., Donard, O.F.X., 2016. Tracing dust transport from Middle-East over Delhi in March 2012 using metal and lead isotope composition. Atmos. Environ. 132, 179–187. https://doi.org/10.1016/j.atmosenv.2016.03.002

Kumar, S., Aggarwal, S.G., Sarangi, B., Malherbe, J., Barre, J.P.G., Berail, S., Séby, F., Donard, O.F.X., 2018. Understanding the Influence of Open-waste Burning on Urban Aerosols using Metal Tracers and Lead Isotopic Composition. Aerosol Air Qual. Res. 18, 2433–2446. https://doi.org/10.4209/aaqr.2017.11.0510

Lamble, K.J., Hill, S.J., 1998. Microwave digestion procedures for environmental matrices . Critical Review. Analyst 123, 103R-133R. https://doi.org/10.1039/A800776D

Lin, Y.-C., Tsai, C.-J., Wu, Y.-C., Zhang, R., Chi, K.-H., Huang, Y.-T., Lin, S.-H., Hsu, S.-C., 2015. Characteristics of trace metals in traffic-derived particles in Hsuehshan Tunnel, Taiwan: size distribution, potential source, and fingerprinting metal ratio. Atmospheric Chem. Phys. 15, 4117–4130. https://doi.org/10.5194/acp-15-4117-2015

Longman, J., Struve, T., Pahnke, K., 2022. Spatial and Temporal Trends in Mineral Dust Provenance in the South Pacific—Evidence From Mixing Models. Paleoceanogr. Paleoclimatology 37, e2021PA004356. https://doi.org/10.1029/2021PA004356

Longman, J., Veres, D., Ersek, V., Phillips, D.L., Chauvel, C., Tamas, C.G., 2018. Quantitative assessment of Pb sources in isotopic mixtures using a Bayesian mixing model. Sci. Rep. 8, 6154. https://doi.org/10.1038/s41598-018-24474-0

Lopez, B., Wang, X., Chen, L.-W.A., Ma, T., Mendez-Jimenez, D., Cobb, L.C., Frederickson, C., Fang, T., Hwang, B., Shiraiwa, M., Park, M., Park, K., Yao, Q., Yoon, S., Jung, H., 2023. Metal contents and size distributions of brake and tire wear particles dispersed in the near-road environment. Sci. Total Environ. 883, 163561. https://doi.org/10.1016/j.scitotenv.2023.163561

Mitra, A., Sen, I.S., Pandey, S.K., Velu, V., Reisberg, L., Bizimis, M., Cloquet, C., Nizam, S., 2021. Lead Isotope Evidence for Enhanced Anthropogenic Particle Transport to the Himalayas during Summer Months. Environ. Sci. Technol. 55, 13697–13708. https://doi.org/10.1021/acs.est.1c03830

NOAA, 2021. GUI Operation © [WWW Document]. URL https://www.ready.noaa.gov/documents/Tutorial_2021/html/test_gui.html (accessed 9.6.24).

O'Neal, M.E., Landis, D.A., Isaacs, R., 2002. An inexpensive, accurate method for measuring leaf area and defoliation through digital image analysis. J. Econ. Entomol. 95, 1190–1194. https://doi.org/10.1603/0022-0493-95.6.1190

Parnell, A.C., Inger, R., Bearhop, S., Jackson, A.L., 2010. Source Partitioning Using Stable Isotopes: Coping with Too Much Variation. PLOS ONE 5, e9672. https://doi.org/10.1371/journal.pone.0009672

Phillips, D.L., Gregg, J.W., 2003. Source partitioning using stable isotopes: coping with too many sources. Oecologia 136, 261–269. https://doi.org/10.1007/s00442-003-1218-3

Phillips, D.L., Koch, P.L., 2002. Incorporating concentration dependence in stable isotope mixing models. Oecologia 130, 114–125. https://doi.org/10.1007/s004420100786

Phillips, D.L., Newsome, S.D., Gregg, J.W., 2005. Combining sources in stable isotope mixing models: alternative methods. Oecologia 144, 520–527. https://doi.org/10.1007/s00442-004-1816-8

PIB, 2023. Joint Military Exercise 'Ex KAVACH' concludes at Andaman and Nicobar Command [WWW Document]. URL https://pib.gov.in/pib.gov.in/Pressreleaseshare.aspx?PRID=1914940 (accessed 12.7.24).

Prakash, V.A.A., 2003. Evolution of the Joint Andaman and Nicobar Command (ANC) and Defence of Our Island Territories [WWW Document]. United Serv. Inst. India. URL https://www.usiofindia.org/publication-journal/evolution-of-the-joint-andaman-and-nicobar-command-anc-and-defence-of-our-island-territories-part-ii.html (accessed 12.7.24).

PTI, 2023. Anti-ship version of BRAHMOS missile successfully test-fired [WWW Document]. URL https://www.brahmos.com/pressRelease.php?id=102 (accessed 12.7.24).

Ray, I., Das, R., Chua, S.L., Wang, X., 2022. Seasonal variation of atmospheric Pb sources in Singapore - Elemental and lead isotopic compositions of PM10 as source tracer. Chemosphere 307, 136029. https://doi.org/10.1016/j.chemosphere.2022.136029

Reuer, M.K., Boyle, E.A., Grant, B.C., 2003. Lead isotope analysis of marine carbonates and seawater by multiple collector ICP-MS. Chem. Geol. 200, 137–153. https://doi.org/10.1016/S0009-2541(03)00186-4

Roser, M., 2021. Data review: how many people die from air pollution? Our World Data.

Sen, I.S., Bizimis, M., Tripathi, S.N., Paul, D., 2016. Lead isotopic fingerprinting of aerosols to characterize the sources of atmospheric lead in an industrial city of India. Atmos. Environ. 129, 27–33. https://doi.org/10.1016/j.atmosenv.2016.01.005

Smith, J.A., Mazumder, D., Suthers, I.M., Taylor, M.D., 2013. To fit or not to fit: evaluating stable isotope mixing models using simulated mixing polygons. Methods Ecol. Evol. 4, 612–618. https://doi.org/10.1111/2041-210X.12048

Stock, B., Jackson, A., Ward, E., Venkiteswaran, J., 2018. brianstock/MixSIAR 3.1.9. https://doi.org/10.5281/zenodo.1209993

Stock, B., Semmens, B., 2016. MixSIAR GUI User Manual v3.1.

Sugiyama, I., Williams-Jones, A.E., 2018. An approach to determining nickel, vanadium and other metal concentrations in crude oil. Anal. Chim. Acta 1002, 18–25. https://doi.org/10.1016/j.aca.2017.11.040

Tessier, A., Campbell, P.G.C., Bisson, M., 1979. Sequential extraction procedure for the speciation of particulate trace metals. Anal. Chem. 51, 844–851. https://doi.org/10.1021/ac50043a017

Tian, H.Z., Zhu, C.Y., Gao, J.J., Cheng, K., Hao, J.M., Wang, K., Hua, S.B., Wang, Y., Zhou, J.R., 2015. Quantitative assessment of atmospheric emissions of toxic heavy metals from anthropogenic sources in China: historical trend, spatial distribution, uncertainties, and control policies. Atmospheric Chem. Phys. 15, 10127–10147. https://doi.org/10.5194/acp-15-10127-2015

UNICEF and Pure Earth, 2020. The toxic truth [WWW Document]. URL https://www.unicef.org/reports/toxic-truth-childrens-exposure-to-lead-pollution-2020 (accessed 3.20.22).

Upadhyay, A., Kanchan, K., Goyal, P.G., Yerramilli, A., Gorai, A.K., 2014. Development of a Fuzzy Pattern Recognition Model for Air Quality Assessment of Howrah City. Aerosol Air Qual. Res. 14, 1639–1652. https://doi.org/10.4209/aaqr.2013.04.0118

Venkataraman, C., Brauer, M., Tibrewal, K., Sadavarte, P., Ma, Q., Cohen, A., Chaliyakunnel, S., Frostad, J., Klimont, Z., Martin, R.V., Millet, D.B., Philip, S., Walker, K., Wang, S., 2018. Source influence on emission pathways and ambient $PM_{2.5}$ pollution over India (2015–2050). Atmospheric Chem. Phys. 18, 8017–8039. https://doi.org/10.5194/acp-18-8017-2018

Wang, Y.Q., Zhang, X.Y., Draxler, R.R., 2009. TrajStat: GIS-based software that uses various trajectory statistical analysis methods to identify potential sources from long-term air pollution measurement data. Environ. Model. Softw. 24, 938–939. https://doi.org/10.1016/j.envsoft.2009.01.004

White, W.M., Albarède, F., Télouk, P., 2000. High-precision analysis of Pb isotope ratios by multi-collector ICP-MS. Chem. Geol. 167, 257–270. https://doi.org/10.1016/S0009-2541(99)00182-5

WHO, 2024. Ambient (outdoor) air pollution [WWW Document]. URL https://www.who.int/news-room/fact-sheets/detail/ambient-(outdoor)-air-quality-and-health (accessed 1.5.25).

Zhang, J., Peng, J., Song, C., Ma, C., Men, Z., Wu, J., Wu, L., Wang, T., Zhang, X., Tao, S., Gao, S., Hopke, P.K., Mao, H., 2020. Vehicular non-exhaust particulate emissions in Chinese megacities: Source profiles, real-world emission factors, and inventories. Environ. Pollut. 266, 115268. https://doi.org/10.1016/j.envpol.2020.115268

Iravati Ray 27.01.2025

Signature of the Candidate with date

Iravati Ray

Registration no.: 1022220001 of 2022

School of Environmental Studies

Jadavpur University

Kolkata-700032

India

Reshmi Das 27/1/25

Reshmi Das, PhD
UGC Assistant Professor
School of Environmental Studies
Jadavpur University
Kolkata-700 032, India

Signature of the Supervisor with date and official seal

Dr. Reshmi Das

UGC Assistant Professor

School of Environmental Studies

Jadavpur University

Kolkata-700032

Sambuddha Misra 27/1/25

Associate Professor
Centre for Earth Sciences
Indian Institute of Science
Bangalore - 560 012, INDIA

Signature of the Supervisor with date and official seal

Dr. Sambuddha Misra

Associate Professor

Centre for Earth Sciences

Indian Institute of Science

Bangalore-560012

India